Automatic Triple-A Segmentation of Skin Cancer Images based on Histogram Classification

Dr. Ahlam Fadhil Mahmood **Hamed Abdulaziz Mahmood**
ahlam.mahmood@gmail.com hamedce43@gmail.com
Computer Engineering Department
University of Mosul

Abstract:

Skin cancer has been the most common and represents 50% of all new cancers detected each year. If detected at an early stage, simple and economic treatment can cure it mostly. Accurate skin lesion segmentation is critical in automated early diagnosis system. This paper present a triple segmentation procedure based on the pixels distribution Bell-shaped (Normal), J-shaped, Reverse J-shaped and U-shaped peaks that is bimodal. According to the nature of dermoscopy images distributions, three segmentation methods are used to identify the normal skin cancer from malignant skin and to extract the tumor region. First, active contours are used for bell distribution shape. Second segmentation is done using adjusted ant colony optimization when the U-shaped peaks distribution was classify. Third segmentation strategies apply adaptive threshold for two J-shapes. Experiments on synthetic and real dermoscopy images demonstrate the advantages of the proposed methods that is able to produce ant colony optimization accurate segmentation when applied to a large number of skin cancer (melanoma) images.

Keyword: Segmentation dermoscopy images, ant colony, active contours, adaptive threshold, Histogram

استقطاع ثلاثي-أ الآلي لسرطان الجلد باعتماد على صنف التوزيع

د.أحلام فاضل محمود **حامد عبد العزيز محمود**
Ahlam.mahmood@gmail.com hamedce43@gmail.com
قسم هندسة الحاسوب
جامعة الموصل

الخلاصة

يعد سرطان الجلد من أكثر أنواع السرطانات انتشارا إذ يشكل نصف الحالات المشخصة للسرطانات سنويا. وحيث أن اكتشافه في المراحل المبكرة يجعل علاجه أسلم وبكلفه أقل. تعتبر عملية استقطاع الجزء المصاب من الجلد صعبة نسبيا لأنظمة التشخيص الآلي المبكر. هذه الورقة تقترح استقطاع ثلاثي ألي حسب توزيع عناصر الصورة توزيع الجرس، توزيع بشكل الحرف جي و معكوسه او توزيع ثنائي القمة. حسب توزيعات الصور المجهرية تم استخدام ثلاث طريق للفصل بين المناطق الطبيعية والمصابة للاستخراج منطقة الورم. أولا، طريقة المحيط الفعال للصور المصنف توزيعها على شكل جرس. ثاني استقطاع تم انجازه باستخدام أمثلية مستعمرة النمل في حالة كون توزيع الصور على شكل حرف يو. ثالث إستراتيجية استقطاع هي العتبة الفعالة لشكلي الحرف جي. التجارب التي اعتمدت الصور المجهرية أكدت فائدة الطرق المقترحة لإمكانيتها في استقطاع دقيق.

Received: 15 – 4 - 2015 **Accepted: 28 – 11 - 2015**

1. Introduction:

Early detection of cancerous skin lesion has been agreed to be very important due to the wide spread of skin cancer as well as the economic and successful treatment if detected early. Malignant melanomas, the deadliest form of all skin cancers, has cure rate of higher than 95% when detected at an early stage[1]. Melanoma incidence rates have been significantly increasing in the last decades, which makes this one of the cancers that has been receiving attention both from the public health field, with medical prevention campaigns, and from the cancer research field[2].

Nowadays, a technique used by dermatologists to diagnose skin lesions and, consequently, to detect melanomas is dermoscopy. Dermoscopy is a method that allows doctors to examine structures in the skin that are not visible to the naked eye. When practiced by experts, dermoscopy improves the diagnostic accuracy of pigmented skin lesions (PSL) [3–5]. Several methods have clinicians interpret the structures revealed through dermoscopy. To measure and detect sets of features from dermoscopic images, the computerized analysis of these images can be extremely useful and helpful for dermatologists in order to facilitate their diagnosis. Based on images obtained by digital dermoscopy, the aims is to develop an aided-diagnostic system for the identification of early stage melanomas. This would enable supervised classification of melanocytic lesions. The melanoma detection process is composed of the follow intuitive steps in a standard pattern recognition processing chain: (a) that are the preprocessing, (b) image segmentation to separate the lesion area from the background skin, (c) extraction of image features for classification purposes, and (d)final classification methods to detection of melanomas and benign in dermoscopy images.

To do a classification of skin lesions must begin by isolating the lesion from healthy skin that surrounds each color image using a segmentation methodology. The detection of this skin lesion is a critical problem in dermatoscopic images because the transition between the lesion and the surrounding skin is difficult to detect accurately. For this, segmentation method chosen must be precise. This paper, proposed a new pixel distribution-based segmentation, which shares the advantages of the active contour model (ACM), ant colony optimization(ACO) and adaptive thresholding technique (ATT). Utilizing the statistical information of the image to apply one of the three models, so it is called triple-A segmentation. The outer part separated to extract melanomas for improves the classification results.

The remainder of the paper is organized as follows. Section 2 provides a description of the previous work. Section 3 explains the three image segmentation methods, the triple-A algorithm. Section 4 describes the experiments results and reports on the findings. Section 4 provides a discussion, and conclusions are drawn in Section 5.

2. Preview of Related Works

In the last decade, several systems for melanoma segmentation and classification have been proposed. Numerous methods have been developed for border detection in dermoscopy images. This non-invasive skin imaging technique involves optical magnification and either liquid immersion and low angle-of-incidence lighting or cross-polarized lighting, making subsurface structures more easily visible when compared to conventional clinical images[6].

Recent approaches include thresholding [2, 6], k-means clustering [7], fuzzy c-means clustering [8, 9], density-based clustering [10], mean shift clustering [11], gradient vector flow snakes [12], color quantization followed by spatial segmentation [13], statistical region merging [14], watershed transformation [15], and supervised learning [16].

In a recent study, K. Zhang et al. [17] demonstrated a region-based active contour model (ACM). The benefits of their method are as follows: first a new region-based signed pressure

force (SPF) function which can efficiently stop the contours at weak or blurred edges. Second, the exterior and interior boundaries can be automatically detected with the initial contour being anywhere in the image. Third, the ACM with SBGFRLS has the property of selective local or global segmentation. It can segment not only the desired object but also the other objects. Fourth, the level set function can be easily initialized with a binary function, which is more efficient to construct than the widely used signed distance function (SDF).

Rahil Garnavi et al. proposed a novel automatic segmentation algorithm using color space analysis and clustering-based histogram thresholding, which is able to find out the optimal color channel for segmentation of skin lesions [13].

J. Yasmin et al. presents a simple yet effective border finding algorithm (improved iterative segmentation algorithm using canny edge detector with iterative filtering) for noisy skin lesions and it compares, its performance with that of the segmentation algorithm using canny detector in the border detection of real noisy skin lesions[18].

In order to automatically separate the lesion from the surrounding normal skin, a triple-A segmentation algorithm depend on the statistical distribution of dermatoscopic images, to detect the border of the lesion, has been developed and discussed in this paper. This algorithm is applied to the image containing the lesion. The proposed algorithm consists of several steps, which are explained below.

3. The Proposed Triple-A Segmentation procedure

The segmentation is the most important stage for analyzing image properly since it affects the accuracy of the subsequent steps. However, proper segmentation is difficult because of the great verities of the lesion shapes, sizes, and colors along with different skin types and textures. In addition, some lesions have irregular boundaries and in some cases there is smooth transition between the lesion and the skin. To address this problem, several algorithms have been proposed. They can be broadly classified as thresholding, edge-based or region-based methods. It consists of several steps, as shown in Figure 1, which are explained next.

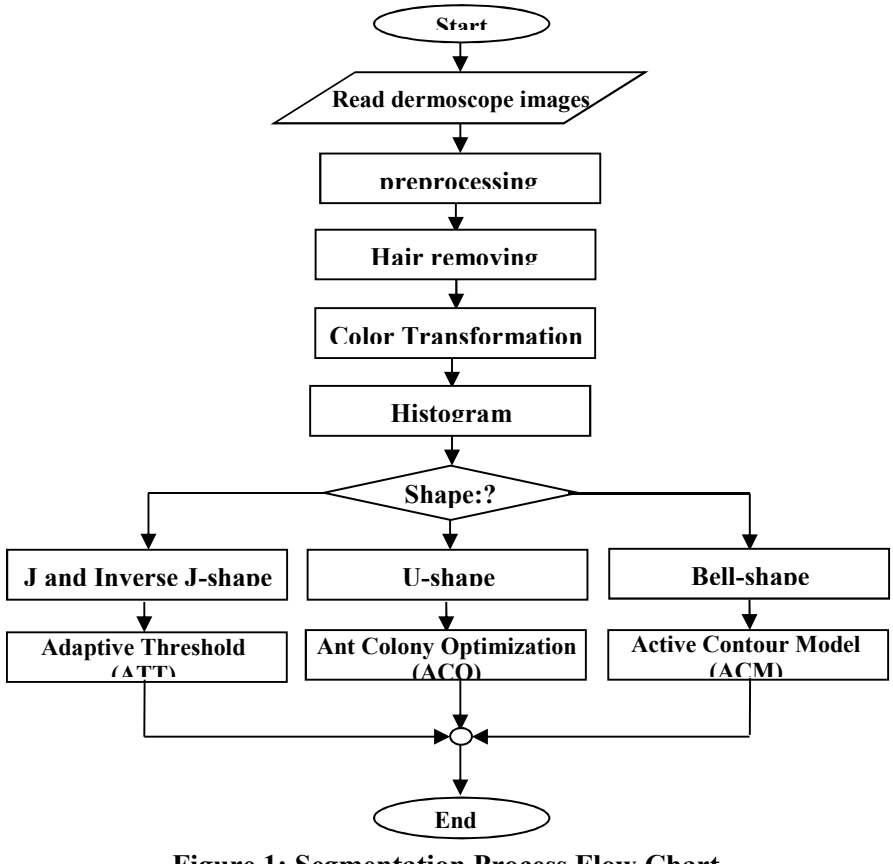

Figure 1: Segmentation Process Flow Chart

3.1 Data Pre processing

120 persons data is collected from different sources where both male and female are present of different age. Obtained data also contains both melanoma non-melanoma patient information. The database images are obtained from different sources, so the size of the images is non-standard. The first step in the process is to resize the image to have a fixed width and height using bicubic interpolation to produce a new image that have a square area of 256 x 256 pixels of all samples.

3.1.1 Hair Removal

Lesions occluded with dark thick hairs can cause problems in the segmentation process. In such cases, the proposed algorithm starts with a hair removal preprocessing, which includes a sequence of steps. These are: (1) localizing dark hairs, bubbles and labels by isolating in mask, (2) using morphological closing operation in vertical, horizontal and diagonal directions, (3) interpolating the removed hair pixels by close non-hair pixels, and (4) smoothing the result using a median filter to eliminate the remaining thin lines.

3.1.2 Color Space Transformation

Thirdly, to suppress large variations within the background and the lesion, and to reduce the effect of different skin their color variations, the original color RGB images are transformed into intensity (grayscale) ones. The separate values of the three color channels (R, G, B) are combined to produce an intensity image (Y) using a commonly accepted transformation, namely $Y = 0.3*R + 0.59*G + 0.11*B$ [13].
rgb2gray converts RGB values to grayscale values by forming a weighted sum of the R, G, and B components: $0.2989 * R + 0.5870 * G + 0.1140 * B$

3.2 Lesion Segmentation-based on the Pixels Distributions

The purpose of this step is separate lesion object and background into non-overlapping sets based on the statistical histogram that is described the image content. However a histogram distributions are well suited to describes different kinds of image present to state the segment method in the proposed triple-A algorithm. Even if specifying a meaningful histogram for a certain dermoscopic images, it is can distinguish as four main obvious shapes, there are some general ones (Gaussian, exponential J, Reverse J-shaped and bimodal U-shape) as demonstrate in figure 2.

For a histogram statistical distribution images, if its histogram has a deep valley between two peaks U-shape. Thus, it is best separate lesion from background using Adjusted Ant Colony Optimization (ACO). As its basic property, ACO tends to achieve a single best route and if there is more than one, it recognizes just one of them. Since edges are not a single solution, automatically solves as well as ants can be stationed on endpoints to gain a higher chance of removing discontinuity[19]. Therefore, this edge detection technique work very well when the image gray-level histogram is bimodal or nearly bimodal. Adaptive Threshold is used for J-distribution or a right skewed histogram, indicating that there were a majority of pixels laying smaller values. As well as histogram that is skewed to the left, that have high intensity pixels. On the other hand, a great deal of images are usually irregularly illuminated leading to a multimodal gaussian histogram (Figure 2) where, in these cases, the ordinary thresholding techniques perform poorly or even fail. In this class of histograms, unlike the bimodal case, there is no clear separation between object and background pixel occurrences. Thus, region-based Active Contour Model (ACM) is useful to used for segmentation. For this

histogram segmentation kinds first, region-based signed pressure force function is used, which can efficiently stop the contours at weak or blurred edges. Second, the exterior and interior boundaries can be automatically detected with the initial contour being anywhere in the image.

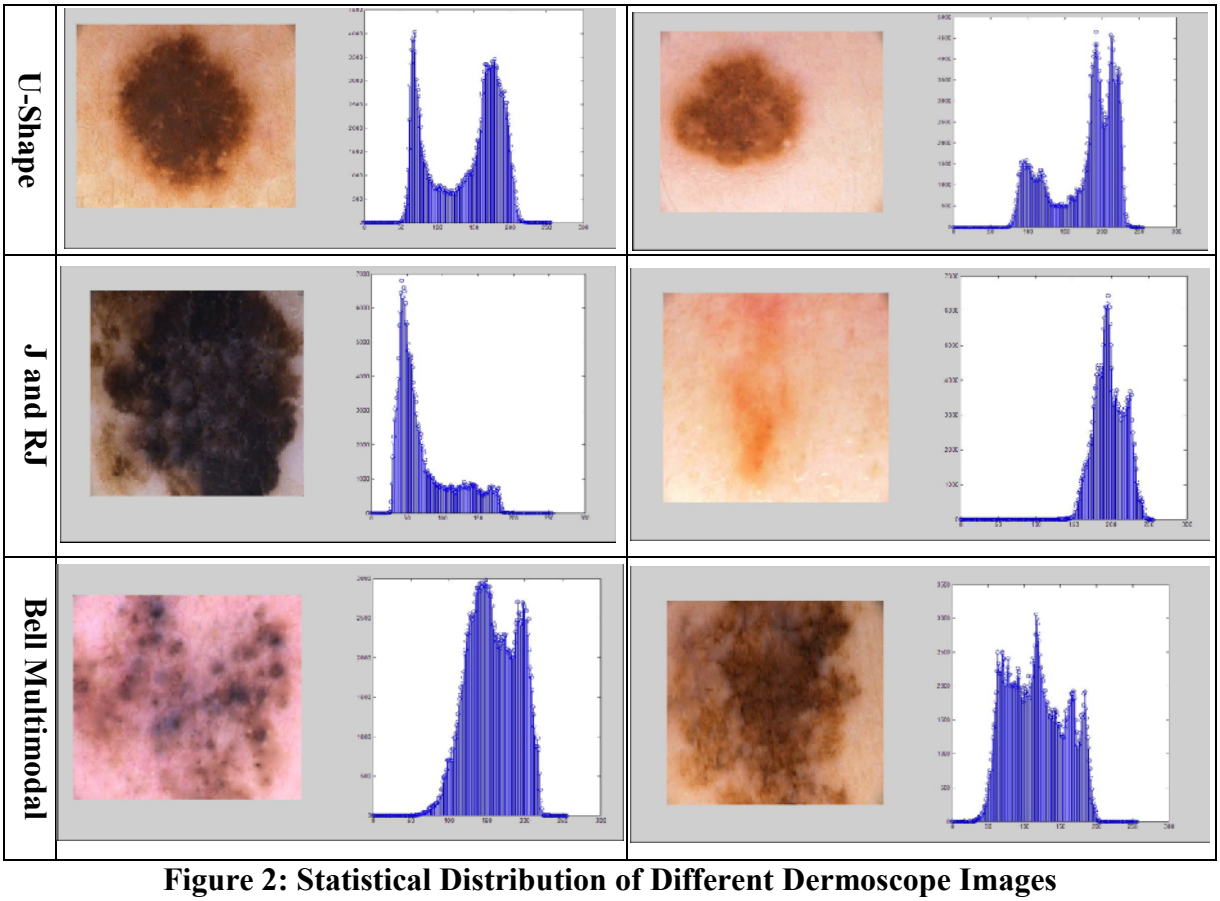

Figure 2: Statistical Distribution of Different Dermoscope Images

3.2.1 Adjusted Ant Colony Optimization (ACO)

ACO has inspired from foraging behavior of real ants. In ACO, a colony of simple agents, called artificial ants, search for good solutions at every generation. Every artificial ant of a generation builds up a solution step by step. These ants, once build a solution, will evaluate the partial solution and deposit some amount of pheromone on the ground in order to communicate between the members of their community which also increases the probability that the other ants will follow the same path (M. Davoodianidaliki et al., 2013). ACO consists of three main components of initial ants' distribution, Node transition rules and pheromone updating rule as state in the following paragraphs:-

A. Initial pheromone value and ants' distribution:

Normally initial pheromone values for every possible node are the same but it's possible to use some basic information to assign initial values. Gradient magnitude matrix is a perfect initial pheromone matrix since it’s a simple assessment of possibility of being on edge for every pixel.

Ants are not initially distributed through whole image randomly but they are divided into two groups. First one is distributed through the magnitude image pixels that are possible edges. Others will be distributed to other parts of image. A few other ants play the role of recognizing all possible pixels of being an edge despite not being on magnitude matrix available. As its basic property, ACO tends to achieve a single best route and if there is more than one, it recognizes just one of them. Since edges are not a single solution, this method automatically solves the problem. Initial ant distribution can also be endpoints of edge image acquired.

B. Transition Rules:

Due to its nature, ACO can be easily fused with Fuzzy without altering process, especially replacing rule. The common rule that determines next stop for every ant is based on probability value computed by Equation 1.

$$P_{i,j} = \frac{{\tau_{i,j}}^{\alpha}{\eta_{i,j}}^{\beta}}{\sum_{\epsilon Ni}{\tau_{i,j}}^{\alpha}{\eta_{i,j}}^{\beta}} \quad \ldots\ldots (1)$$

Where τ_{ij} is pheromone linking node i to j, η_{ij} is heuristic information between nodes i and j, α, β represents relative influence of pheromone and heuristic information in selection process. A few options are provided to compute heuristic information such as equation 4. In which I is a function that gives an estimation of neighbor pixel relations and can be any of equations 5-8 or similar ones. x is gray value.

$$\eta_{i,j} = \frac{1}{z} V_c(I_{i,j}) \quad \ldots\ldots (2)$$

Where Z=$Z = \sum_{i=1:M1}\sum_{j=1:M2} V_c(I_{i,j})$, which is a normalization factor, $I_{i,j}$ is the intensity value of the pixel at the position (i,j) of the image I, the function$V_c(I_{i,j})$ is a function of a local group of pixels c (called the clique), and its value depends on the variation of intensity values on the clique c (as shown in Figure 3), the function $V_c(I_{i,j})$ mentioned in [20] is

$$\begin{aligned} V_c(I_{i,j}) = f(&|I_{i-2,j-1} - I_{i+2,j+1}| + |I_{i-2,j+1} - I_{i+2,j-1}| + |I_{i-1,j-2} - I_{i+1,j+2}| \\ &+ |I_{i-1,j-1} - I_{i+1,j+1}| + |I_{i-1,j} - I_{i+1,j}| + |I_{i-1,j+1} - I_{i+1,j-1}| \\ &+ |I_{i-1,j+2} - I_{i-1,j-2}| + |I_{i,j-1} - I_{i,j+1}| \end{aligned} \quad \ldots\ldots (3)$$

Final step in transition rule is the death of ant that occurs by arriving to one of its previous pixels. There is option of dynamic neighbourhood in which ant can escape death based on a 50% chance once by increasing neighbourhood pixels from 8 to 12 (Figure 3).

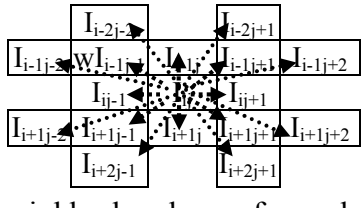

Figure 3. Increasing neighborhood once for each ant to 8 or 12 pixels.

C. Pheromone update rule:

There are two update processes in each generation of ants. When every ant meets its end, according to attributes of the path it has gone, pheromone value of the travelled path is updated. Also when all ants of one generation die, pheromone is evaporated.

$$\tau_{i,j} = (1-\rho)\tau_{i,j} + \sum_{k=1}^{m} \Delta\tau_{i,j}^{k} \quad \ldots\ldots (4)$$

In which ρ is pheromone evaporation rate and m is number of ants.

$$\Delta\tau_{i,j}^{k} = \frac{Q}{L_k} \quad \ldots\ldots (5)$$

Q is a constant and L_k is the length measured by k^{th} ant.

D. Decision Process:

In this step, a binary decision is made at each pixel location to determine whether it is edge or not, by applying a threshold on the final pheromone matrix. The initial threshold T_0 is selected as the mean value of the pheromone matrix. Next, the entries of the pheromone matrix is classified into two categories according to the criterion that its value is lower than T_0 or larger than T_0. Then the new threshold is computed as the average of two mean values of each of above two categories. The above process is repeated until the threshold value does not change any more.

3.2.2 Adaptive Threshold Technique (ATT)

J or reverse J skin image histogram, the segmentation is done by using an adaptive thresholding algorithm, which comprises three steps: 1) histogram computation; 2) peak detection; and 3) threshold estimation.

First, the input image is converted into a gray-level image by selecting the channel with the highest entropy [2]. Then, the histogram of intensity, i.e., h(i), i = 0, . . . , 255, is computed constant.

Then extract the most significant peaks of the histogram. If the histogram has a single peak located at i_1, the threshold is defined by $T = i_1 + \Delta T$. The ΔT offset was empirically tuned and set to 15. If two significant peaks are extracted, the threshold was choose that corresponds to the maximum valley. The valley is defined as follows: Given two peaks located at i_1, i_2, ($i_2 > i_1$), then define the valley at i as the difference between the straight line draw by the peaks and the histogram amplitude at i as illustrated in Figure 4.

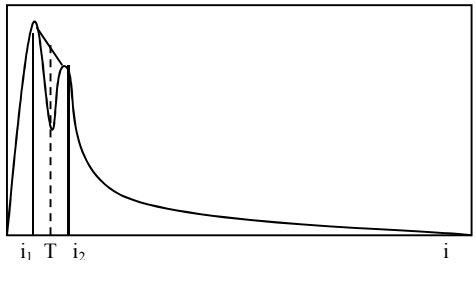

Figure 4: Threshold computation
In the case of two peaks

The only information missing is how to select the most significant peaks in a histogram if more than two peaks are detected . It is involves two steps. First, close peaks are merged and replaced by a single peak, i.e., the largest one. Consider that two peaks located at i_1 and i_2 are close if $|i1 - i2| < \Delta i$ ($\Delta i = 8$). If the number of peaks is larger than 2 after this step, the highest peak is selected. Then, all the remaining ones are tested. The second selected peak is the one that corresponds to the largest depth of the valley between two histogram peaks.

3.2.3 Active Contours Model(ACM)

Region-based ACMs have many advantages over edge-based ones. First, region-based models utilize the statistical information inside and outside the contour to control the evolution, which are less sensitive to noise and have better performance for images with weak edges or without edges. Second, they are significantly less sensitive to the location of initial contour and then can efficiently detect the exterior and interior boundaries simultaneously.

One of the most popular region-based models are the C–V and GAC models. So to segment a multimodal bell histogram which was distribute major pixels on wide range, shares the advantages of the C–V and GAC models for utilizing the statistical information inside and outside the contour to construct a region-based signed pressure force (SPF) function[17]. The main procedures of the proposed algorithm are summarized as follows:

1. Initialize the level set function ϕ as

$$\phi(x, t=0) = \begin{cases} 0 & x \in \partial\Omega_0 \\ +\rho & x \in \Omega - \Omega_0 \end{cases} \quad \ldots\ldots(6)$$

where $\rho > 0$ is a constant, Ω_0 is a subset in the image domain Ω and $\partial\Omega_0$ is the boundary of Ω_0.

2. Compute $c_1(\phi)$ and $c_2(\phi)$, where c_1 and c_2 are two constants which are the average intensities inside and outside the contour for a given image I in domain Ω,

$$c_1(\phi) = \frac{\int_\Omega I(x).H(\phi)dx}{\int_\Omega H(\phi)dx} \quad \ldots\ldots(7)$$

$$C_2 = \frac{\int_\Omega I(x).(1-H(\phi))dx}{\int_\Omega (1-H(\phi))dx} \quad \ldots\ldots(8)$$

Where $H(\phi)$ is the Heaviside function

3. Evolve the level set function according to the following Equation

$$\frac{\partial\phi}{\partial t} = spf(I(x)).\alpha|\nabla\phi|, \quad x \in \Omega. \quad \ldots\ldots(9)$$

$$spf(I(x)) = \frac{I(x) - \frac{C_1 + C_2}{2}}{\max(\left|I(x) - \frac{C_1 + C_2}{2}\right|)}, \quad x \in \Omega. \quad \ldots\ldots(10)$$

where α constant velocity term a is added to increase the propagation speed and ∇ is the gradient operator.

4. Let $\phi = 1$ if $\phi > 0$; otherwise, $\phi = -1$.

5. Regularize the level set function with a Gaussian filter, i.e. $\phi = \phi * G_\sigma$.

6. Check whether the evolution of the level set function has converged if not, return to step 2.

3.3 Experimental results

The hybrid segmentation approach is implemented in Matlab R2013a on a 2.GHz 2GHz Intel(R) core(TM)2 Duo CPU. In the experiment, the dermatoscopic image suspected as melanoma is used as input data. To evaluate the performance of our developed system, this research use dataset of 120 dermatocospic images. The adaptive threshold used in each experiment, we choose $\rho = 1$, $\varepsilon = 1.5$, $\sigma = 1$, $K = 5$, and time step $\Delta t = 1$. The values of α were set according to the images. The segmented of the dermatoscopic images results are shown in Figure 5 for different cases.

Cases	Dermoscopy Images	Ground Truth Images	ACO Segmentation	ATT Segmentation	ACM Segmentation
1-7 ATT	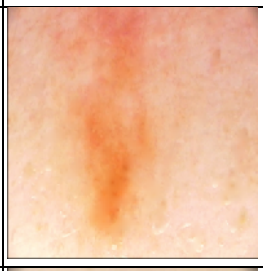		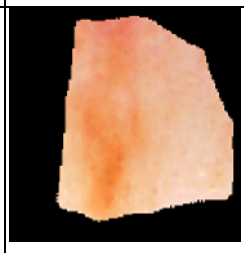		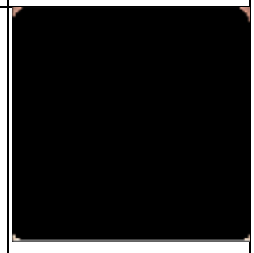
2-67 ATT	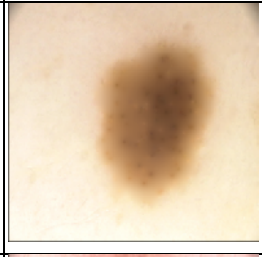				
3-65 active			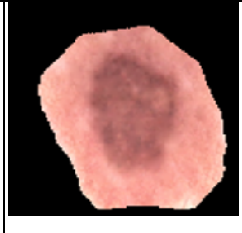	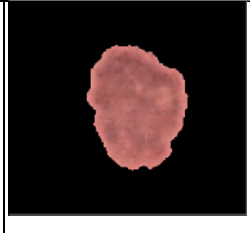	
4-51 Ant	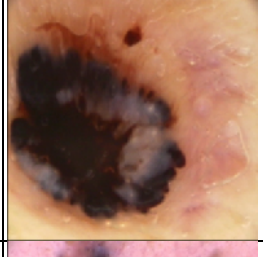				
5-200 active	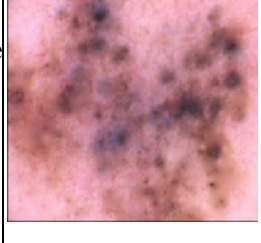	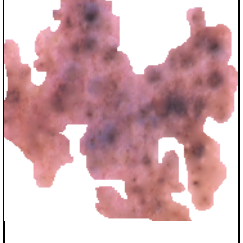	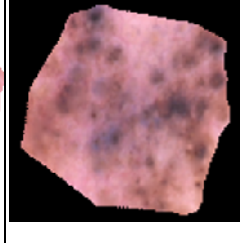	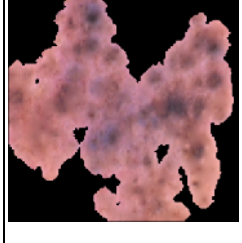	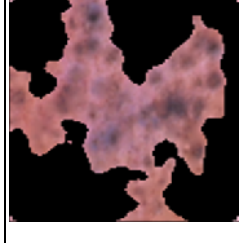
6-196 Ant		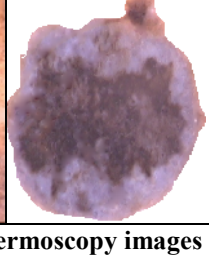	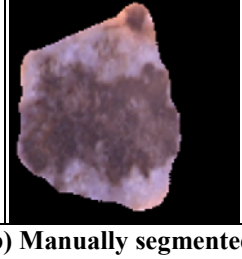	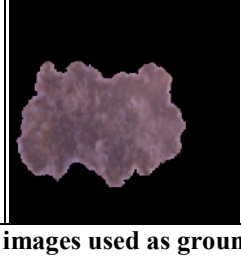	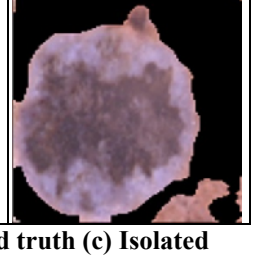

Figure 5: (a) Original Skin Dermoscopy images (b) Manually segmented images used as ground truth (c) Isolated Skin Lesion regions of the segmented images using ACO method (d) Segmented by ATT (e) ACM

The measures used for the evaluation of the hybrid segmentation are accuracy, sensibility and specificity measures presented as follows,

$$S_e = \frac{Tp}{Tp+FN} \times 100\% \quad \text{.....(11)}$$

$$S_P = \frac{Tp}{TN+FP} \times 100\% \quad \text{.....(12)}$$

$$A_{cc} = \frac{Tp+TN}{Tp+FN+TN+FP} \times 100\% \quad \text{.....(13)}$$

Where TP is the number of true positives, FN the number of false negatives, TN the number of true negative, and FP the number of false positives. The experimental results of total dermatocospy images is described in Table 1.

Table 1: Segmentation Performance of the Proposed Methods

Cases	Methods	TP	FN	FP	TN	Sensitivity	Specificity	ACC	Computational cost
1	ATT	111462	6276	11982	132424	94.6	91.7	93.03	low
2	ATT	160770	12093	24696	64585	93	72.3	85.9	low
3	ATT	38883	798	13185	209278	97.9	94.07	94.6	low
4	ATT	108132	1140	24576	128296	98.9	83.9	90.1	low
5	ATT	97203	17352	3393	144196	84.8	97.7	92.08	low
6	ATT	232857	173778	2316	146807	57.2	98.4	68.3	low
7	ATT	143640	55185	57	63262	72.2	99.9	78.9	low
8	ACO	187157	13678	14107	47202	93.1	76.9	89.4	high
9	ACO	284531	33622	10104	66113	89.4	86.7	88.9	high
10	ACO	140613	10449	5429	105653	93.08	95.1	93.9	high
11	ACO	286852	12731	9963	47402	95.7	82.6	93.6	high
12	ACO	118337	25684	4863	113260	82.1	95.8	88.3	high
13	ACO	255366	42828	10016	46066	85.6	82.10	85.08	high
14	ACO	295013	14752	40823	88444	95.2	68.4	87.3	medium
15	ACM	101566	151847	4845	3886	40.07	44.5	40.2	medium
16	ACM	122349	427461	1711	289377	22.2	99.4	48.9	medium
17	ACM	196529	60139	13160	7684	76.5	36.8	73.5	medium
18	ACM	114693	262653	1500	116702	30.3	98.7	46.6	medium
19	ACM	394126	124697	1949	258628	75.9	99.2	83.70	medium
20	ACM	244316	8686	27385	18243	96.5	39.9	87.9	medium

4. Conclusion

This paper has presented an automated approach for lesion segmentation based on the histogram classification. The proposed method is tested on a set of 120 dermoscopy images, this procedure combines advantages of three methods employed are Ant Colony Optimization that's better solution for to U pixels distributions, which ants detect lesions border well. And Adaptive Thresholds Technique if the histogram skewed to the right as well as to the left. Third histogram kinds that's have bell multimodal distribution which possesses the property of local or global segmentation.

Segmentation results are quantitatively evaluated by comparing automated results to manual segmented lesions independently drawn by dermatologists. The comparison is done with respect to four different metrics of accuracy, sensitivity, specificity and computational cost. Experimental results indicate that ATT and ACM obtain the highest overall

performance with an accuracy. The results are also compared with two other automated methods, which demonstrate that the proposed perform well on all images with a different lesion kinds. Adaptive thresholding-based method, in spite of its simplicity, with a proper choice of suggested color channels is highly competitive with the well-known skin lesion segmentation methods, and outperforms them with respect to accuracy, specificity, and Acc metrics. Furthermore, the proposed ACO is potentially slower since it is try to update the pheromone values in such a way that the probability to generate high-quality solutions increases over time.

For the future, the developed procedure hence provides a useful tool as a first stage in the automatic classification melanoma of skin lesion images. Moreover, perform the experiments on a large dermoscopy image set and also to investigate more evaluation metrics.

References:-

[1]J. Abdul Jaleel, S. Salim and Aswin.R.B, "Artificial Neural Network Based Detection of Skin Cancer", International Journal of Advanced Research in Electrical, Electronics and Instrumentation Engineering, Vol. 1, Issue 3, pp.200-205, September 2012.(1.686)

[2]C. Barata, M. Ruela, M. Francisco, T. Mendonça and J. S. Marques, "Two Systems for the Detection of Melanomas in Dermoscopy Images Using Texture and Color Features", IEEE Systems Journal, Volume: PP, Issue: 99, pp.1-15, 29 July 2013.(1.2)

[3]M. Zortea, T. R. Schopf, K. Thon, M. Geilhufe, K. Hindberg, H. Kirchesch, K. Møllersen, J. Schulz, S. O. Skrøvseth and F. Godtliebsen, "A Performance of a Dermoscopy-Based Computer Vision System for the Diagnosis of Pigmented Skin Lesions Compared with Visual Evaluation by Experienced Dermatologists", Artificial Intelligence in Medicine 60 pp.13–26, 2014. (1.767).

[4]M. Sadeghi, T. Lee, D. Mclean, H. Lui and M. S. Atkins, "Detection and Analysis of Irregular Streaks in Dermoscopic Images of Skin Lesions", IEEE Transactions On Medical Imaging, VOL. 32, NO. 5,pp. 849 -861, MAY 2013. (4.027)

[5] N. Smaoui and S. Bessassi, "A developed system for melanoma diagnosis", International Journal of Computer Vision and Signal Processing, 3(1), pp.10-17, 2013.(3.623)

[6] M. E. Celebi, Q. Wen, S. Hwang, H. Iyatomi and G. Schaefer, "Lesion Border Detection in Dermoscopy Images Using Ensembles of Thresholding Methods", Skin Research and Technology, 19(1): e252-e258, 2013. (1.409)

[7] K. Ahmed, T. Jesmin and Z. Rahman, "Early Prevention and Detection of Skin Cancer Risk using Data Mining", International Journal of Computer Applications (0975 – 8887) Volume 62– No.4, January 2013.

[8] L. P. Suresh, K. L. Shunmuganathan and S. H. Krishna, "Dermoscopic Image Segmentation using Machine Learning Algorithm", American Journal of Applied Sciences 8 (11): pp.1159-1168, 2011.

[9]H. Lee and Y. P. Chen, "Skin cancer extraction with optimum fuzzy thresholding technique", Applied Intelligence April 2014, Volume 40, Issue 3, pp 415-426, 2014.

[10]A. H. Bhuiyan, I. Azad and K. Uddin, "Image Processing for Skin Cancer Features Extraction", International Journal of Scientific & Engineering Research Vol. 4, Issue 2, ISSN 2229-5518, pp.1-6, February-2013.

[11] H. Zhou, G. Schaefer, A. Sadka, and M. Celebi, "Anisotropic Mean Shift Based Fuzzy C-Means Segmentation of Dermoscopy Images", IEEE Journal of Selected Topics in Signal Processing, VOL. 3, NO. 1,pp.26-34, February 2009.

[12] K. A. Mahmoud and A. Al-Jumaily, "Segmentation of Skin Cancer Images Based on Gradient Vector Flow (GVF) Snake", Proceedings of the 2011 IEEE International Conference on Mechatronics and Automation August 7 - 10, Beijing, China, 2011.
[13]R. Garnavi, M. Aldeen, M. E. Celebi, A. Bhuiyan, C. Dolianitis, and G. Varigos, "Automatic Segmentation of Dermoscopy Images Using Histogram Thresholding on Optimal Color Channels", World Academy of Science, Engineering and Technology 55, pp.1040-1048, 2011.
[14]M. E. Celebi, H. A. Kingravi, H. Iyatomi, J. Lee, Y. A. Aslandogan, W. V. Stoecke, R. Moss, J. M. Malters and A. A. Marghoob, "Fast and Accurate Border Detection in Dermoscopy Images Using Statistical Region Merging", Medical Imaging 2007: Image Processing, edited by Josien P. W. Pluim, Joseph M. Reinhardt, Proc. of SPIE Vol. 6512, 65123V-1, (2007).
[15] H. Wang, X. Chen, R. H. Moss, R. J. Stanley, W. V. Stoecker, M. E. Celebi, T. M. Szalapski, J. M. Malters, J. M. Grichnik, A. A. Marghoob, H. S. Rabinovitz and S. W. Menzies, "Watershed segmentation of dermoscopy images using a watershed technique", Skin Research and Technology, 16(3): 378–384, pp.1-17, August 2010.
[16] M. Elgamal, "Automatic Skin Cancer Images Classification", (IJACSA) International Journal of Advanced Computer Science and Applications, Vol. 4, No. 3, pp. 287- 294, 2013.
[17] K. Zhang, L. Zhang, H. Song, W. Zhou, "Active contours with selective local or global segmentation: A new formulation and level set method", Image and Vision Computing 28, pp. 668–676, 2010.
[18]J. H. Jaseema Yasmin, M. Mohamed Sadiq, "An Improved Iterative Segmentation Algorithm using Canny Edge Detector with Iterative Median Filter for Skin Lesion Border Detection", International Journal of Computer Applications (0975 – 8887) Volume 50 – No.6, pp.37-42, July 2012.
[19]M. Davoodianidaliki, A. Abedin, M. Shankayi, "Adaptive Edge Detection using Adjusted Ant Colony Optimization", Remote Sensing and Spatial Information Sciences, Volume XL-1/W3, Tehran, Iran, 2013.
[20] J. Tian, W. Yu, and S. Xie, "An Ant Colony Optimization Algorithm For Image Edge Detection",

The work was carried out at the college of Engineering. University of Mosul